Supporting Information for Moreau, Schubert, Nasr, Török, Miller, Kennedy, Kemp:

"Context-Independent, Temperature-Dependent Helical Propensities for Amino Acid Residues."

I. Circular Dichroism Data

A. Norleucine scan

peptide 2	$-[\theta]_{222}$ deg cm^2 dmol^{-1}		
	2°C	25°C	60°C
$WK_4Inp_2{}^tLNleA_{18}{}^tLInp_2K_4NH_2$	27844	18765	7750
$WK_4Inp_2{}^tLANleA_{17}{}^tLInp_2K_4NH_2$	28975	18341	7394
$WK_4Inp_2{}^tLA_2NleA_{16}{}^tLInp_2K_4NH_2$	27579	18217	7233
$WK_4Inp_2{}^tLA_3NleA_{15}{}^tLInp_2K_4NH_2$	30339	20298	8120
$WK_4Inp_2{}^tLA_5NleA_{13}{}^tLInp_2K_4NH_2$	27816	19068	7813
$WK_4Inp_2{}^tLA_7NleA_{11}{}^tLInp_2K_4NH_2$	28620	18815	7444
$WK_4Inp_2{}^tLA_9NleA_9{}^tLInp_2K_4NH_2$	28872	18798	7728
$WK_4Inp_2{}^tLA_{11}NleA_7{}^tLInp_2K_4NH_2$	28243	18134	7322
$WK_4Inp_2{}^tLA_{13}NleA_5{}^tLInp_2K_4NH_2$	28316	18422	7357
$WK_4Inp_2{}^tLA_{15}NleA_3{}^tLInp_2K_4NH_2$	28851	18590	7627
$WK_4Inp_2{}^tLA_{16}NleA_2{}^tLInp_2K_4NH_2$	27745	17947	7405
$WK_4Inp_2{}^tLA_{17}NleA{}^tLInp_2K_4NH_2$	27900	18124	7598
$WK_4Inp_2{}^tLA_{18}Nle{}^tLInp_2K_4NH_2$	29162	19212	7728

B. Double Norleucine scan

	2°C	25°C	60°C
$WK_4Inp_2^tLA_9Nle_2A_8^tLInp_2K_4NH_2$	28066	17309	7466
$WK_4Inp_2^tLA_8NleANleA_8^tLInp_2K_4NH_2$	27573	17264	7204
$WK_4Inp_2^tLA_8NleA_2NleA_7^tLInp_2K_4NH_2$	26489	16843	7342
$WK_4Inp_2^tLA_7NleA_3NleA_7^tLInp_2K_4NH_2$	29313	19404	8408
$WK_4Inp_2^tLA_6NleA_4NleA_7^tLInp_2K_4NH_2$	28321	17664	7353
$WK_4Inp_2^tLA_5NleA_7NleA_5^tLInp_2K_4NH_2$	28223	18262	7671
$WK_4Inp_2^tLA_2NleA_{13}NleA_2^tLInp_2K_4NH_2$	27398	18080	7725

C. Double Norvaline scan

	2°C	25°C	60°C
$WK_4Inp_2^tLA_9Nva_2A_8^tLInp_2K_4NH_2$	26089	15519	6596
$WK_4Inp_2^tLA_8NvaANvaA_8^tLInp_2K_4NH_2$	26211	15650	6610
$WK_4Inp_2^tLA_8NvaA_2NvaA_7^tLInp_2K_4NH_2$	24274	14660	6161
$WK_4Inp_2^tLA_7NvaA_3NvaA_7^tLInp_2K_4NH_2$	27222	17311	7330
$WK_4Inp_2^tLA_6NvaA_4NvaA_7^tLInp_2K_4NH_2$	26698	16166	6999
$WK_4Inp_2^tLA_5NvaA_7NvaA_5^tLInp_2K_4NH_2$	27092	16638	7023
$WK_4Inp_2^tLA_2NvaA_{13}NvaA_2^tLInp_2K_4NH_2$	26442	16915	7171

D. Single and double Guests $WK_4Inp_2{}^tLNleA_9XA_9{}^tLInp_2K_4NH_2$ $WK_4Inp_2{}^tLNleA_9X_2A_8{}^tLInp_2K_4NH_2$

$-[\theta]_{222}$ deg cm^2 $dmol^{-1}$ Guest X

Guest	2°C	25°C	60°C	double Guest	2°C	25°C	60°C
Pro	1346	2406	3236				
Gly	12828	7127	4285	GG	3925	3568	3429
Val	21366	12056	5719	VV	13509	7157	4419
Phe	22617	12688	5288	FF	13438	7372	4048
Ser-OMe	23835	13322	5385	$(S\text{-}OMe)_2$	17349	8590	4203
Ile	24035	14578	6303	II	19289	10906	5681
Met	24048	14855	6374	MM	20615	12601	5888
Abu	26323	16123	6485	Abu_2	23103	13006	5486
Leu	26162	16701	7073	7357	24143	15092	6813
Ala	27464	17757	6825	7627	27464	15519	6825
Nva	27791	17353	7247	Nva_2	27464	17757	6596
Nle	28872	18798	7728	Nle_2	28066	17697	7466
Asn	18993	10685	5302	NN	10252	6488	4622
Ser	19920	10912	4726	SS	11317	6517	4710
Thr	20549	11057	5551	TT	9513	4551	4386
Tyr	20930	12220	5533	YY	11922	6979	3715
Gln	23943	14152	6232	QQ	17266	10021	4760

E. Lysine pH 7, Arginine pH 7, Histidine pH 1.2

peptide 2 $-[\theta]_{222}$ deg cm^2 $dmol^{-1}$

	2°C	25°C	60°C
$WK_4Inp_2{}^tLLysA_{18}{}^tLInp_2K_4NH_2$	24035	14436	6123
$WK_4Inp_2{}^tLALysA_{17}{}^tLInp_2K_4NH_2$	23168	13484	6189
$WK_4Inp_2{}^tLA_2LysA_{16}{}^tLInp_2K_4NH_2$	22857	13453	5889
$WK_4Inp_2{}^tLA_3LysA_{15}{}^tLInp_2K_4NH_2$	23532	13375	5754
$WK_4Inp_2{}^tLA_9LysA_9{}^tLInp_2K_4NH_2$	25582	14866	6154
$WK_4Inp_2{}^tLA_{11}LysA_7{}^tLInp_2K_4NH_2$	24997	14817	6566
$WK_4Inp_2{}^tLA_{13}LysA_5{}^tLInp_2K_4NH_2$	26565	16622	7198
$WK_4Inp_2{}^tLA_{15}LysA_3{}^tLInp_2K_4NH_2$	27835	18293	8021
$WK_4Inp_2{}^tLA_{16}LysA_2{}^tLInp_2K_4NH_2$	27371	18382	8043
$WK_4Inp_2{}^tLA_{17}NleA{}^tLInp_2K_4NH_2$	28597	19703	8678
$WK_4Inp_2{}^tLA_{18}Lys{}^tLInp_2K_4NH_2$	29284	20029	8328
$WK_4Inp_2{}^tLArgA_{18}{}^tLInp_2K_4NH_2$	22419	13118	4994
$WK_4Inp_2{}^tLA_4ArgA_{14}{}^tLInp_2K_4NH_2$	22006	12016	4421
$WK_4Inp_2{}^tLA_9ArgA_9{}^tLInp_2K_4NH_2$	24321	14644	5296
$WK_4Inp_2{}^tLA_{12}ArgA_6{}^tLInp_2K_4NH_2$	26244	16623	6571
$WK_4Inp_2{}^tLA_{15}ArgA_3{}^tLInp_2K_4NH_2$	27013	18068	7266
$WK_4Inp_2{}^tLA_{18}Arg{}^tLInp_2K_4NH_2$	28142	19271	7604
$WK_4Inp_2{}^tLA_4HisA_{14}{}^tLInp_2K_4NH_2$	17611	9046	3177
$WK_4Inp_2{}^tLA_9HisA_9{}^tLInp_2K_4NH_2$	17620	9259	3374
$WK_4Inp_2{}^tLA_{12}HisA_6{}^tLInp_2K_4NH_2$	26244	16623	6008
$WK_4Inp_2{}^tLA_{15}HisA_3{}^tLInp_2K_4NH_2$	27013	18068	7266
$WK_4Inp_2{}^tLA_{18}His{}^tLInp_2K_4NH_2$	27733	18800	8642
$WK_4Inp_2{}^tLA_9GluA_9{}^tLInp_2K_4NH_2$	26364	14162	6232 pH 1.2
$WK_4Inp_2{}^tLA_9GluA_9{}^tLInp_2K_4NH_2$	26539	16360	6609 pH 7
$WK_4Inp_2{}^tLA_9AspA_9{}^tLInp_2K_4NH_2$	20929	11438	4694 pH 1.2
$WK_4Inp_2{}^tLA_9AspA_9{}^tLInp_2K_4NH_2$	23174	12986	6198 pH 7

F. Double and Triple Lysine scan

	2°C	25°C	60°C
$WK_4Inp_2{}^tLA_8K_3A_8{}^tLInp_2K_4NH_2$	10510	6154	6072
$WK_4Inp_2{}^tLA_7KAKAKA_7{}^tLInp_2K_4NH_2$	7263	4673	5463
$WK_4Inp_2{}^tLA_6KA_2KA_2KA_6{}^tLInp_2K_4NH_2$	5638	4039	5100
$WK_4Inp_2{}^tLA_5KA_3KA_3KA_5{}^tLInp_2K_4NH_2$	6874	4583	5920
$WK_4Inp_2{}^tLA_4KA_4KA_4KA_4{}^tLInp_2K_4NH_2$	12273	7030	6561
$WK_4Inp_2{}^tLA_6KA_5KA_6{}^tLInp_2K_4NH_2$	18159	10835	7799
$WK_4Inp_2{}^tLA_8KAKA_8{}^tLInp_2K_4NH_2$	18018	10015	6897

II. Molecular Ion MS Data for Series 2 Peptides

Peptide	*m/z* Found (Expected)
NleA14	753.26 (752.48), 602.80 (602.19), 502.52 (501.99), 430.90 (430.42), 377.17 (376.75)
ANleA13	753.23 (752.48), 602.78 (602.19), 502.52 (501.99), 430.88 (430.42), 377.06 (376.75)
A2NleA12	1003.98 (1002.98), 753.38 (752.48), 602.80 (602.19), 502.52 (501.99), 430.90 (430.42), 377.17 (376.75)
A3NleA11	1003.98 (1002.98), 753.26 (752.48), 602.80 (602.19), 502.52 (501.99), 430.90 (430.42), 377.17 (376.75)
A5NleA9	753.16 (752.48), 602.72 (602.19), 502.52 (501.99), 430.81 (430.42), 377.00 (376.75)
A7NleA7	1003.79 (1002.98), 753.38 (752.48), 602.87 (602.19), 502.52 (501.99), 430.96 (430.42), 377.17 (376.75)
A9NleA5	753.45 (752.48), 602.93 (602.19), 502.71 (501.99), 430.96 (430.42), 377.17 (376.75)
A11NleA3	753.23 (752.48), 602.85 (602.19), 502.52 (501.99), 430.88 (430.42), 377.19 (376.75), 251.66 (251.50)
A12NleA2	602.52 (602.19), 502.26 (501.99), 430.68 (430.42), 376.86 (376.75), 251.46 (251.50)
A13NleA	1003.85 (1002.98), 753.52 (752.48), 602.80 (602.19), 502.52 (501.99), 430.90 (430.42), 377.17 (376.75)
A14Nle	1004.17 (1002.98), 753.20 (752.48), 602.80 (602.19), 502.58 (501.99), 430.90 (430.42), 377.11 (376.75)
NleA18	659.55 (659.02), 549.82 (549.35), 471.34 (471.02), 412.52 (412.26)
ANleA17	659.62 (659.02), 549.82 (549.35), 471.34 (471.02), 412.65 (412.26)
A2NleA16	659.55 (659.02), 550.02 (549.35), 471.47 (471.02), 412.72 (412.26)
A3NleA15	824.43 (823.52), 659.77 (659.02), 549.95 (549.35), 471.54 (471.02), 412.76 (412.26)
A5NleA13	549.95 (549.35), 471.54 (471.02), 412.72 (412.26)
A7NleA11	659.69 (659.02), 549.95 (549.35), 471.54 (471.02), 412.65 (412.26)
A2NleA13NleA2	667.81 (667.43), 556.43 (556.36), 477.09 (477.02), 417.56 (417.52)
A5NleA7NleA5	668.07 (667.43), 556.81 (556.36), 477.53 (477.02), 417.94 (417.52)
A6NleA4NleA6	668.01 (667.43), 556.81 (556.36), 477.47 (477.02), 417.88 (417.52)

A7NleA3NleA7	667.94 (667.43), 556.75 (556.36), 477.35 (477.02), 417.82 (417.52)
A8NleA2NleA7	668.07 (667.43), 556.81 (556.36), 477.53 (477.02), 417.94 (417.52)
A8NleANleA8	667.62 (667.43), 556.43 (556.36), 477.09 (477.02), 417.56 (417.52)
A9NleNleA8	668.07 (667.43), 556.94 (556.36), 477.47 (477.02), 418.01 (417.52)
A2NvaA13NvaA2	662.08 (661.82), 551.88 (551.69), 473.22 (473.02), 414.20 (414.02)
A5NvaA7NvaA5	827.42 (827.03), 662.08 (661.82), 551.88 (551.69), 473.22 (473.02), 414.20 (414.02)
A6NvaA4NvaA6	827.55 (827.03), 662.26 (661.82), 551.94 (551.69), 473.35 (473.02), 414.26 (414.02)
A7NvaA3NvaA7	827.55 (827.03), 662.14 (661.82), 551.94 (551.69), 473.22 (473.02), 414.20 (414.02)
A8NvaA2NvaA7	827.98 (827.03), 662.58 (661.82), 552.32 (551.69), 473.60 (473.02), 414.51 (414.02)
A8NvaANvaA8	827.36 (827.03), 662.14 (661.82), 551.94 (551.69), 473.16 (473.02), 414.20 (414.02)
A9NvaNvaA8	827.74 (827.03), 662.45 (661.82), 552.19 (551.69), 473.41 (473.02), 414.38 (414.02)
A9NvaA9	820.76 (820.02), 656.78 (656.22), 547.52 (547.01), 469.42 (469.01), 410.89 (410.51), 365.39 (365.01)
A9ValValA8	828.17 (827.03), 662.51 (661.82), 552.32 (551.69), 473.60 (473.02), 414.51 (414.02)
A9ValA9	820.88 (820.02), 656.90 (656.22), 547.58 (547.01), 469.55 (469.01), 410.95 (410.51)
A9AbuAbuA8	820.94, 656.90, 547.52, 469.48, 410.89, 365.39
A9AbuA9	817.20, 653.97, 545.15, 467.43, 409.08, 363.83
A9LeuLeuA8	835.03 (83), 668.12 (667.43), 556.87 (556.36), 477.46 (477.02), 417.94 (417.52)
A9LeuA9	824.25 (823.52), 659.52 (659.02), 549.76 (549.35), 471.42 (471.02), 412.57 (412.26)
A9IleIleA8	835.03 (834.03), 668.25 (667.43), 556.99 (556.36), 477.59 (477.02), 418.06 (417.52)
A9IleA9	824.18 (823.52), 659.46 (659.02), 549.70 (549.35), 471.29 (471.02), 412.51 (412.26)

A9MetMetA8	843.69 (843.01), 675.10 (674.61), 562.79 (562.34), 482.51 (482.15), 422.30 (422.01)
A9MetA9	828.79 (828.01), 663.26 (662.61), 552.88 (552.34), 474.03 (473.58), 414.94 (414.51)
A9PhePheA8	681.33 (681.02), 567.92 (567.69), 486.96 (486.73), 426.27 (426.02)
A9PheA9	666.69 (665.82), 555.62 (555.01), 476.46 (475.87), 417.06 (416.51)
A9TyrTyrA8	687.56 (687.42), 573.02 (573.14), 491.43 (491.30), 430.10 (430.02)
A9TyrA9	836.76 (836.02), 669.71 (669.01), 558.13 (557.68), 478.56 (478.16), 418.88 (418.51)
A9AsnAsnA8	556.93 (556.68), 477.46 (477.30), 417.94 (417.76)
A9AsnA9	659.71 (659.21), 549.89 (549.51), 471.42 (471.15), 412.64 (412.38)
A9SerSerA8	657.59 (657.01), 548.14 (547.67), 469.98 (469.58), 411.39 (411.01)
A9SerA9	654.22 (653.81), 545.29 (545.01), 467.49 (467.29), 409.20 (409.01)
A9ThrThrA8	552.82 (552.35), 473.97 (473.58), 414.88 (414.51)
A9ThrA9	820.79 (820.51), 656.83 (656.61), 547.53 (547.34), 469.41(469.30), 410.86 (410.76)
A9GlnGlnA8	673.79 (673.42), 561.65 (561.35), 481.58 (481.30), 421.51 (421.26)
A9GlnA9	551.94 (551.85), 473.22 (473.15)
A9GlyGlyA8	806.57 (806.00), 645.44 (645.00), 538.10 (537.67), 461.37 (461.00), 403.83 (403.50)
A9GlyA9	648.43 (647.81), 540.64 (540.01), 463.53 (463.01), 405.75 (405.26)
A9ProA9	820.03 (819.51), 656.26 (655.81), 547.02 (546.68), 468.97 (468.73), 410.55 (410.26)
LysA18	552.26 (551.85), 473.53 (473.16), 414.38 (414.14)
ALysA17	552.26 (551.85), 473.53 (473.16), 414.44 (414.14)
A2LysA16	662.07 (662.02), 551.95 (551.85), 473.13 (473.16), 414.21 (414.14)
A3LysA15	552.32 (551.85), 473.66 (473.16), 414.57 (414.14)
HisA18	829.95 (829.51), 664.21 (663.81), 553.65 (553.35), 474.71 (474.44), 415.47 (415.26)
A4HisA14	829.76 (829.51), 664.03 (663.81), 553.46 (553.35), 474.52 (474.44), 415.41 (415.26)

A9HisA9	830.01 (829.51), 664.15 (663.81), 553.59 (553.35), 474.71 (474.44), 415.54 (415.26)
A12HisA6	829.69 (829.51), 663.90 (663.81), 553.46 (553.35), 474.52 (474.44), 415.28 (415.26)
A15HisA3	829.76 (829.51), 664.09 (663.81), 553.52 (553.35), 474.59 (474.44), 415.41 (415.26)
A18His	830.20 (829.51), 664.40 (663.81), 553.78 (553.35), 474.84 (474.44), 415.60 (415.26)
A9HisHisA8	846.51 (846.02), 677.48 (677.02), 564.71 (564.35), 484.23 (483.87), 423.87 (423.51), 376.92 (376.57)
ArgA18	834.87 (834.28), 668.13 (667.62), 556.93 (556.52), 477.55 (477.16)
A4ArgA14	834.93 (834.28), 668.13 (667.62), 556.93 (556.52), 477.55 (477.16)
A9ArgA9	667.753 (667.62), 556.62 (556.52), 477.24 (477.16), 417.68 (417.64)
A12ArgA6	834.87 (834.28), 668.07 (667.62), 556.93 (556.52), 477.55 (477.16)
A15ArgA3	834.49 (834.28), 667.75 (667.62), 556.56 (556.52), 477.24 (477.16), 417.68 (417.64)
A18Arg	834.49 (834.28), 667.88 (667.62), 556.68 (556.52), 477.37 (477.16), 417.81 (417.64)
A9ArgArgA8	685.18 (684.63), 571.08 (570.70), 489.68 (489.31), 428.61 (428.27)
A9AspAspA8	835.82 (835.00), 668.82 (668.21), 557.57 (557.01), 478.06 (477.58),
A9AspA9	824.83 (824.01), 660.05 (659.41), 550.18 (549.67), 471.81 (471.29)
A9GluGluA8	842.76 (842.01), 674.38 (673.81), 562.18 (561.68), 482.04 (481.58), 421.91 (421.51)
A9GluA9	828.30 (827.51), 662.89 (662.21), 552.51 (552.01), 473.77 (473.30), 414.65 (414.26)
A9S(OMe)S(OMe)A8	828.88 (828.01), 663.32 (662.61), 552.82 (552.35), 474.17 (473.58), 415.05 (414.51)
A9S(OMe)A9	821.05 (820.51), 656.99 (656.61), 547.70 (547.34), 469.58(469.30), 411.08 (410.76)

III. ^{13}C=O NMR-derived Data and MS Data for Series 1 Peptides

Table 1. Helical propensities assigned from ^{13}C=O chemical shifts in ^{t}L-Ala$_9$-Xxx-Ala$_9$-tL at 2°C.

	Helical Propensity at T = 2°C		*^{13}C=O Chemical Shift*		
Amino Acid	*∅ w_{Xxx}*	*SD*	*Site 12*	*Site 14*	*Site 15*
Ala	1.56	-	180.576	180.261	179.995
Nle	1.49	0.06	180.563	180.261	179.986
Nva	1.47	0.05	180.564	180.287	179.991
Glu	1.22	0.21	180.476	180.247	179.947
Leu	1.10	0.20	180.448	180.229	179.926
Arg	0.87	0.04	180.435	180.123	179.881
Met	0.87	0.06	180.398	180.142	179.885
Ile	0.78	0.02	180.389	180.087	179.858
Gln	0.68	0.07	180.288	180.082	179.826
Lys	0.67	0.06	180.357	180.036	179.807
Asp	0.56	0.04	180.247	180.000	179.757
Val	0.55	0.02	180.242	179.981	179.757
Trp	0.53	0.08	180.142	180.005	179.752
Phe	0.52	0.08	180.146	180.004	179.734
Tyr	0.50	0.09	180.105	180.000	179.716
Ser	0.45	0.07	180.151	179.931	179.633
Asn	0.37	0.04	180.041	179.835	179.579
Cys	0.37	0.02	180.032	179.821	179.611
Thr	0.36	0.02	180.050	179.817	-
His	0.18	0.02	179.624	179.441	179.258
Gly	0.17	0.02	179.592	179.377	179.212
Pro	0.013	0.004	178.237	179.201	178.324

Table 2. Helical propensities assigned from ^{13}C=O chemical shifts in ^{t}L-Ala$_9$-Xxx-Ala$_9$-tL at 25°C.

	Helical Propensity at T = 25°C		*^{13}C=O Chemical Shift*		
Amino Acid	*∅ w_{Xxx}*	*SD*	*Site 12*	*Site 14*	*Site 15*
Ala	1.39	-	179.734	179.391	179.144
Nle	1.37	0.06	179.707	179.405	179.139
Nva	1.20	0.05	179.643	179.350	179.098
Leu	1.15	0.10	179.597	179.354	179.079
Glu	1.00	0.07	179.546	179.290	179.015
Met	0.90	0.03	179.473	179.221	178.997
Ile	0.81	0.03	179.418	179.176	178.956
Arg	0.80	0.04	179.450	179.153	178.933
Gln	0.72	0.03	179.327	179.121	178.906
Trp	0.64	0.07	179.208	179.089	178.851
Lys	0.60	0.04	179.276	179.006	178.814
Asp	0.54	0.03	179.199	178.965	178.764
Val	0.53	0.03	179.162	178.970	178.764
Ser	0.51	0.03	179.144	178.951	178.732
Phe	0.50	0.04	179.075	178.960	178.754
Tyr	0.50	0.04	179.066	178.965	178.750
Asn	0.43	0.04	179.038	178.846	178.663
Thr	0.40	0.02	178.988	178.823	-
Cys	0.36	0.01	178.892	178.759	178.608
Gly	0.22	0.02	178.613	178.471	178.361
His	0.20	0.02	178.562	178.448	178.324
Pro	0.045	0.01	177.949	177.926	177.972

Table 3. Helical propensities assigned from $^{13}C=O$ chemical shifts in $^{t}L\text{-}Ala_9\text{-}Xxx\text{-}Ala_9\text{-}tL$ at 60°C.

	Helical Propensity at T = 60°C		*$^{13}C=O$ Chemical Shift*		
Amino Acid	*$\varnothing w_{Xxx}$*	*SD*	*Site 12*	*Site 14*	*Site 15*
Nle	1.24	0.04	178.178	178.026	177.889
Leu	1.22	0.05	178.159	178.022	177.885
Ala	1.17	-	178.159	177.999	177.857
Nva	1.14	0.03	178.127	177.985	177.857
Glu	1.04	0.01	178.086	177.949	177.817
Met	0.99	0.04	178.036	177.921	177.816
Ile	0.98	0.05	178.017	177.917	177.811
Asp	0.94	0.03	178.045	177.875	177.770
Trp	0.92	0.07	177.962	177.903	177.793
Gln	0.86	0.04	177.958	177.866	177.766
Ser	0.83	0.03	177.944	177.848	177.752
Val	0.78	0.04	177.894	177.834	177.734
Asn	0.75	0.05	177.926	177.784	177.720
Tyr	0.72	0.06	177.830	177.811	177.715
Phe	0.72	0.06	177.830	177.807	177.715
Thr	0.71	0.02	177.848	177.788	-
Arg	0.70	0.03	177.880	177.770	177.688
Lys	0.67	0.02	177.853	177.756	177.679
Cys	0.59	0.03	177.734	177.734	177.660
Gly	0.51	0.02	177.724	177.660	177.614
Pro	0.31	0.03	177.541	177.541	177.541
His	0.31	0.01	177.546	178.546	177.509

Table 4. Relative free energies with standard deviations for the twenty naturally occurring amino acids plus norleucine and norvaline measured in ^{t}L-Ala$_9$-Xxx-Ala$_9$-^{t}L, covering the temperature range of 2, 25, and 60°C.

Amino Acid	*T = 2°C*		*T = 25°C*		*T = 60°C*	
	ΔΔG	*SD*	*ΔΔG*	*SD*	*ΔΔG*	*SD*
Ala	0.00	0.00	0.00	0.00	0.00	0.00
Nle	0.02	0.02	0.01	0.03	-0.04	0.02
Nva	0.03	0.02	0.09	0.03	0.02	0.02
Glu	0.14	0.09	0.19	0.04	0.08	0.00
Leu	0.19	0.09	0.11	0.05	-0.03	0.03
Arg	0.32	0.03	0.33	0.03	0.34	0.03
Met	0.32	0.04	0.26	0.02	0.11	0.03
Ile	0.38	0.02	0.32	0.02	0.12	0.04
Gln	0.45	0.06	0.39	0.03	0.20	0.03
Lys	0.46	0.05	0.50	0.03	0.37	0.02
Asp	0.56	0.04	0.56	0.04	0.15	0.02
Val	0.57	0.02	0.57	0.03	0.26	0.04
Trp	0.59	0.08	0.46	0.06	0.16	0.05
Phe	0.60	0.08	0.60	0.05	0.33	0.06
Tyr	0.63	0.10	0.60	0.05	0.30	0.06
Ser	0.69	0.09	0.59	0.04	0.23	0.02
Asn	0.79	0.07	0.69	0.03	0.29	0.05
Cys	0.78	0.03	0.79	0.02	0.46	0.06
Thr	0.79	0.06	0.74	0.06	0.33	0.04
His	1.17	0.06	1.16	0.06	0.88	0.02
Gly	1.22	0.06	1.10	0.05	0.55	0.04
Pro	2.63	0.18	2.03	0.13	0.85	0.09

Table 5. Chemical Shift Scan at 2, 25, and 60°C for the Series of Hydrophobic Guests in Ala_{19}: W-K_6-$^tL_3$-A_9-*Xxx*-A_9-$^tL_3$-K_6-NH_2; *Xxx* = Ala, Nva, Val

Site ^{13}C=O Label	*Chemical shift (ppm) measured at the Indicated Temperature*								
	Ala			*Nva*			*Val*		
	2°C	*25°C*	*60°C*	*2°C*	*25°C*	*60°C*	*2°C*	*25°C*	*60°C*
1	178.109	177.656	176.969	178.091	177.619	176.928	178.013	177.500	176.910
2	179.597	178.722	177.560	179.580	178.640	177.514	179.221	178.278	177.408
3	179.817	178.960	177.697	179.859	178.878	177.669	179.441	178.452	177.518
4	180.224	179.258	177.862	180.151	179.121	177.775	179.743	178.649	177.614
5	180.499	179.537	177.999	180.385	179.372	177.917	179.899	178.773	177.651
6	180.590	179.675	178.086	180.325	179.372	177.949	179.569	178.645	177.660
7	180.654	179.771	178.168	180.710	179.752	178.159	180.384	179.153	177.766
8	180.709	179.844	178.210	180.499	179.643	178.127	179.977	178.970	177.729
9	180.723	179.885	178.242	180.755	179.913	178.315	180.650	179.459	178.063
10	180.705	179.881	178.228	180.302	180.421	-	180.302	179.176	177.802
11	180.673	179.821	178.223	180.242	180.316	Table 3	180.242	179.162	177.894
12	180.576	179.734	178.159	180.045	180.132	-	180.045	179.038	177.871
14	180.261	179.391	177.999	179.981	180.004	Table 3	179.981	178.970	177.834
15	179.995	179.144	177.857	179.757	179.739	Table 3	179.757	178.764	177.734
17	178.384	177.903	177.267	179.359	179.327	-	179.359	178.471	177.587
18	177.702	177.473	177.088	178.301	178.237	-	178.301	177.775	177.221
19	177.477	177.340	177.051	177.683	177.633	-	177.683	177.418	177.065

Table 6. Chemical Shift Scan at 2, 25, and 60°C for the Series of Hydrophobic Guests in Ala_{19}: W-K_6-$^tL_3$-A_9-*Xxx*-A_9-$^tL_3$-K_6-NH_2; *Xxx* = Leu, Nle, Ile

Site ^{13}C=O Label	*Chemical shift (ppm) measured at the Indicated Temperature*								
	Leu			*Nle*			*Ile*		
	2°C	*25°C*	*60°C*	*2°C*	*25°C*	*60°C*	*2°C*	*25°C*	*60°C*
1	178.095	177.628	176.960	178.114	177.656	176.969	177.990	177.518	176.891
2	179.473	178.594	177.509	179.542	178.658	177.523	179.272	178.420	177.431
3	179.743	178.823	177.665	179.807	178.906	177.697	179.510	178.567	177.540
4	180.087	179.116	177.834	180.183	179.208	177.848	179.826	178.809	177.656
5	180.279	179.295	177.930	180.407	179.441	177.976	180.018	179.020	177.756
6	180.206	179.258	177.949	180.384	179.423	177.990	179.858	178.864	177.729
7	180.728	179.844	178.297	180.696	179.826	178.232	180.522	179.459	177.917
8	180.467	179.638	178.205	180.549	179.716	178.182	180.160	179.263	177.875
9	180.934	180.027	178.406	180.810	180.027	178.411	180.824	179.748	178.168
10	180.609	179.720	178.168	180.663	179.784	178.173	180.430	179.455	177.917
11	180.448	179.597	178.159	180.563	179.707	178.178	180.389	179.418	178.017
12	180.302	179.464	178.100	180.375	179.546	178.113	180.174	179.276	177.985
14	180.229	179.354	178.022	180.261	179.405	178.026	180.087	179.176	177.917
15	179.926	179.079	177.885	179.986	179.139	177.889	179.858	178.956	177.811
17	179.519	178.718	177.701	179.583	178.777	177.701	179.492	178.635	177.642
18	178.356	177.894	177.276	178.393	177.917	177.280	178.338	177.853	177.253
19	177.702	177.473	177.102	177.711	177.477	177.097	177.702	177.459	177.083

Table 7. ^{13}C=O Labeling and Mass Spec Data for $^{t}L_3$-A_9-*Xxx*-A_9-$^{t}L_3$; *Xxx* = 20 Natural Amino Acids plus Nle, Nva

Note: Every peptide synthesized in this study was C-terminally amidated.

Peptide Sequence	*Site ^{13}C=O Label*	*Percent ^{13}C=O Label*	*Average MW (Da)*	*[m+zH]/z Expected*					*[m+zH]/z Observed*				
				4	*5*	*6*	*7*	*8*	*4*	*5*	*6*	*7*	*8*
Xxx = 20 Natural Amino Acids plus Nle, Nva													
W-K_6-$^{t}L_3$-A_9-A-A_9-$^{t}L_3$-K_6	12,14,15	100/75/50	3772.78	943.62	755.10	629.42	539.64	472.31	944.00	756.00	630.00	540.00	472.00
W-K_6-$^{t}L_3$-A_9-C-A_9-$^{t}L_3$-K_6	12,14,15	100/75/50	3804.84	951.61	761.49	634.74	544.21	476.31	952.00	762.00	635.00	544.00	476.00
W-K_6-$^{t}L_3$-A_9-D-A_9-$^{t}L_3$-K_6	12,14,15	100/75/50	3816.79	954.62	763.90	636.75	545.93	477.81	955.00	764.00	637.00	546.00	478.00
W-K_6-$^{t}L_3$-A_9-E-A_9-$^{t}L_3$-K_6	12,14,15	100/75/50	3830.81	958.12	766.70	639.08	547.93	479.56	959.00	767.00	639.00	548.00	480.00
W-K_6-$^{t}L_3$-A_9-F-A_9-$^{t}L_3$-K_6	12,14,15	100/75/50	3848.87	962.63	770.30	642.09	550.51	481.82	963.00	771.00	643.00	551.00	482.00
W-K_6-$^{t}L_3$-A_9-G-A_9-$^{t}L_3$-K_6	12,14,15	100/75/50	3758.75	940.12	752.29	627.08	537.64	470.56	940.00	753.00	627.00	538.00	471.00
W-K_6-$^{t}L_3$-A_9-H-A_9-$^{t}L_3$-K_6	12,14,15	100/75/50	3838.84	960.13	768.30	640.42	549.08	480.57	961.00	768.00	641.00	550.00	481.00
W-K_6-$^{t}L_3$-A_9-I-A_9-$^{t}L_3$-K_6	12,14,15	100/75/50	3814.86	954.13	763.51	636.42	545.65	477.57	955.00	764.00	637.00	546.00	478.00
W-K_6-$^{t}L_3$-A_9-K-A_9-$^{t}L_3$-K_6	12,14,15	100/75/50	3829.87	957.88	766.51	683.93	547.79	479.45	958.00	767.00	640.00	548.00	480.00
W-K_6-$^{t}L_3$-A_9-L-A_9-$^{t}L_3$-K_6	12,14,15	100/75/50	3814.86	954.13	763.51	636.42	545.65	477.57	954.00	764.00	636.00	546.00	478.00
W-K_6-$^{t}L_3$-A_9-M-A_9-$^{t}L_3$-K_6	12,14,15	100/75/50	3832.90	958.62	767.10	639.42	548.22	479.81	959.00	767.00	640.00	549.00	480.00
W-K_6-$^{t}L_3$-A_9-N-A_9-$^{t}L_3$-K_6	12,14,15	100/75/50	3815.80	954.37	763.70	636.58	545.79	477.69	955.00	764.00	637.00	546.00	478.00
W-K_6-$^{t}L_3$-A_9-P-A_9-$^{t}L_3$-K_6	12,14,15	100/75/50	3798.81	950.12	760.30	633.75	543.36	475.57	951.00	761.00	634.00	544.00	476.00
W-K_6-$^{t}L_3$-A_9-Q-A_9-$^{t}L_3$-K_6	12,14,15	100/75/50	3829.83	957.88	766.50	638.92	547.79	479.44	958.00	767.00	639.00	548.00	479.00
W-K_6-$^{t}L_3$-A_9-R-A_9-$^{t}L_3$-K_6	12,14,15	100/75/50	3857.88	964.89	772.11	643.59	551.80	482.95	965.00	772.00	644.00	552.00	483.00
W-K_6-$^{t}L_3$-A_9-S-A_9-$^{t}L_3$-K_6	12,14,15	100/75/50	3788.78	947.62	758.30	632.08	541.93	474.31	948.00	758.00	632.00	542.00	475.00
W-K_6-$^{t}L_3$-A_9-T-A_9-$^{t}L_3$-K_6	12,14,16	100/75/50	3802.80	951.12	761.10	634.42	543.93	476.07	951.00	761.00	635.00	544.00	477.00
W-K_6-$^{t}L_3$-A_9-V-A_9-$^{t}L_3$-K_6	12,14,15	100/75/50	3800.83	950.63	760.70	634.09	543.65	475.82	951.00	761.00	634.00	544.00	476.00
W-K_6-$^{t}L_3$-A_9-W-A_9-$^{t}L_3$-K_6	12,14,15	100/75/50	3887.91	972.38	778.11	648.59	556.08	486.69	972.00	778.00	649.00	556.00	487.00
W-K_6-$^{t}L_3$-A_9-Y-A_9-$^{t}L_3$-K_6	12,14,15	100/75/50	3864.87	966.63	773.50	644.75	552.79	483.82	967.00	774.00	645.00	553.00	484.00
W-K_6-$^{t}L_3$-A_9-Nle-A_9-$^{t}L_3$-K_6	12,14,15	100/75/50	3814.86	954.13	763.51	636.42	545.65	477.57	955.00	764.00	637.00	545.00	478.00
W-K_6-$^{t}L_3$-A_9-Nva-A_9-$^{t}L_3$-K_6	12,14,15	100/75/50	3800.83	950.63	760.70	634.09	543.65	475.82	951.00	761.00	635.00	544.00	476.00

Table 8. $^{13}C=O$ Labeling and Mass Spec Data for Chemical Shift Scans of $^{t}L_3$-A_9-*Xxx*-A_9-$^{t}L_3$; *Xxx* = Ala, Ile

Note: Every peptide synthesized in this study was C-terminally amidated.

Peptide Sequence	*Site $^{13}C=O$ Label*	*Percent $^{13}C=O$ Label*	*Average MW (Da)*	*[m+zH]/z Expected*					*[m+zH]/z Observed*				
				4	*5*	*6*	*7*	*8*	*4*	*5*	*6*	*7*	*8*
Xxx = Ala													
W-K_6-$^{t}L_3$-A_9-A-A_9-$^{t}L_3$-K_6	1,4,7	100/80/60	3772.78	943.62	755.10	629.42	539.64	472.31	944.00	756.00	630.00	540.00	472.00
W-K_6-$^{t}L_3$-A_9-A-A_9-$^{t}L_3$-K_6	2,5,8	25/50/100	3772.78	943.62	755.10	629.42	539.64	472.31	944.00	756.00	630.00	540.00	472.00
W-K_6-$^{t}L_3$-A_9-A-A_9-$^{t}L_3$-K_6	3,6,9	25/50/100	3772.78	943.62	755.10	629.42	539.64	472.31	944.00	756.00	630.00	540.00	472.00
W-K_6-$^{t}L_3$-A_9-A-A_9-$^{t}L_3$-K_6	3,10,19	25/50/100	3772.78	943.62	755.10	629.42	539.64	472.31	944.00	756.00	630.00	540.00	472.00
W-K_6-$^{t}L_3$-A_9-A-A_9-$^{t}L_3$-K_6	11,14,17	25/50/100	3772.78	943.62	755.10	629.42	539.64	472.31	944.00	756.00	630.00	540.00	472.00
W-K_6-$^{t}L_3$-A_9-A-A_9-$^{t}L_3$-K_6	12,15,18	25/50/100	3772.78	943.62	755.10	629.42	539.64	472.31	944.00	756.00	630.00	540.00	472.00
W-K_6-$^{t}L_3$-A_9-A-A_9-$^{t}L_3$-K_6	13,15,17	25/50/100	3772.78	943.62	755.10	629.42	539.64	472.31	944.00	756.00	630.00	540.00	472.00
Xxx = Ile													
W-K_6-$^{t}L_3$-A_9-I-A_9-$^{t}L_3$-K_6	1,4,7	25/50/100	3814.86	954.13	763.51	636.42	545.65	477.57	955.00	764.00	637.00	546.00	478.00
W-K_6-$^{t}L_3$-A_9-I-A_9-$^{t}L_3$-K_6	2,5,8	25/50/100	3814.86	954.13	763.51	636.42	545.65	477.57	955.00	764.00	637.00	546.00	478.00
W-K_6-$^{t}L_3$-A_9-I-A_9-$^{t}L_3$-K_6	3,6,9	25/50/100	3814.86	954.13	763.51	636.42	545.65	477.57	955.00	764.00	637.00	546.00	478.00
W-K_6-$^{t}L_3$-A_9-I-A_9-$^{t}L_3$-K_6	11,14,17	25/50/100	3814.86	954.13	763.51	636.42	545.65	477.57	955.00	764.00	637.00	546.00	478.00
W-K_6-$^{t}L_3$-A_9-I-A_9-$^{t}L_3$-K_6	12,15,18	25/50/100	3814.86	954.13	763.51	636.42	545.65	477.57	955.00	764.00	637.00	546.00	478.00
W-K_6-$^{t}L_3$-A_9-I-A_9-$^{t}L_3$-K_6	13,16,19	25/50/100	3814.86	954.13	763.51	636.42	545.65	477.57	955.00	764.00	637.00	546.00	478.00

Table 9. $^{13}C=O$ Labeling and Mass Spec Data for Chemical Shift Scans of $^{t}L_3$-A_9-*Xxx*-A_9-$^{t}L_3$; *Xxx* = Leu, Nle, Nva, Val

Note: Every peptide synthesized in this study was C-terminally amidated.

Peptide Sequence	*Site $^{13}C=O$ Label*	*Percent $^{13}C=O$ Label*	*Average MW (Da)*	*[m+zH]/z Expected*					*[m+zH]/z Observed*				
				4	*5*	*6*	*7*	*8*	*4*	*5*	*6*	*7*	*8*
Xxx = Leu													
W-K_6-$^{t}L_3$-A_9-L-A_9-$^{t}L_3$-K_6	1,4,7	25/50/100	3814.86	954.13	763.51	636.42	545.65	477.57	954.00	764.00	637.00	546.00	478.00
W-K_6-$^{t}L_3$-A_9-L-A_9-$^{t}L_3$-K_6	2,5,8	25/50/100	3814.86	954.13	763.51	636.42	545.65	477.57	954.00	764.00	637.00	546.00	478.00
W-K_6-$^{t}L_3$-A_9-L-A_9-$^{t}L_3$-K_6	3,6,9	25/50/100	3814.86	954.13	763.51	636.42	545.65	477.57	954.00	764.00	637.00	546.00	478.00
W-K_6-$^{t}L_3$-A_9-L-A_9-$^{t}L_3$-K_6	11,14,17	25/50/100	3814.86	954.13	763.51	636.42	545.65	477.57	954.00	764.00	637.00	546.00	478.00
W-K_6-$^{t}L_3$-A_9-L-A_9-$^{t}L_3$-K_6	12,15,18	25/50/100	3814.86	954.13	763.51	636.42	545.65	477.57	954.00	764.00	637.00	546.00	478.00
W-K_6-$^{t}L_3$-A_9-L-A_9-$^{t}L_3$-K_6	13,16,19	25/50/100	3814.86	954.13	763.51	636.42	545.65	477.57	954.00	764.00	637.00	546.00	478.00
Xxx = Nle													
W-K_6-$^{t}L_3$-A_9-Nle-A_9-$^{t}L_3$-K_6	1,3,5,7,9	20/40/60/80/100	3816.86	954.63	763.91	636.76	545.94	477.82	955.00	764.00	637.00	546.00	478.00
W-K_6-$^{t}L_3$-A_9-Nle-A_9-$^{t}L_3$-K_6	2,4,6,8	25/50/75/100	3815.85	954.38	763.71	636.59	545.79	477.70	954.00	764.00	637.00	546.00	478.00
W-K_6-$^{t}L_3$-A_9-Nle-A_9-$^{t}L_3$-K_6	12,14,16,18	25/50/75/100	3815.85	954.38	763.71	636.59	545.79	477.70	954.00	764.00	637.00	546.00	478.00
W-K_6-$^{t}L_3$-A_9-Nle-A_9-$^{t}L_3$-K_6	11,13,15,17,19	20/40/60/80/100	3816.86	954.63	763.91	636.76	545.94	477.82	955.00	764.00	637.00	546.00	478.00
Xxx = Nva													
W-K_6-$^{t}L_3$-A_9-Nva-A_9-$^{t}L_3$-K_6	1,4,9	25/50/100	3800.83	950.63	760.70	634.09	543.65	475.82	951.00	761.00	634.00	544.00	476.00
W-K_6-$^{t}L_3$-A_9-Nva-A_9-$^{t}L_3$-K_6	2,4,6,8	25/50/75/100	3801.83	950.88	760.90	634.26	543.79	475.94	951.00	761.00	635.00	544.00	476.00
W-K_6-$^{t}L_3$-A_9-Nva-A_9-$^{t}L_3$-K_6	2,3,5,6,7	20/40/60/80/100	3802.84	951.13	761.11	634.42	543.93	476.07	952.00	761.00	634.00	544.00	476.00
W-K_6-$^{t}L_3$-A_9-Nva-A_9-$^{t}L_3$-K_6	8,12,14,16,18	20/40/60/80/100	3802.84	951.13	761.11	634.42	543.93	476.07	952.00	761.00	634.00	544.00	476.00
W-K_6-$^{t}L_3$-A_9-Nva-A_9-$^{t}L_3$-K_6	11,13,15,17,19	20/40/60/80/100	3802.84	951.13	761.11	634.42	543.93	476.07	952.00	761.00	634.00	544.00	476.00
Xxx = Val													
W-K_6-$^{t}L_3$-A_9-V-A_9-$^{t}L_3$-K_6	1,4,9	25/50/100	3800.83	950.63	760.70	634.09	543.65	475.82	951.00	761.00	634.00	544.00	476.00
W-K_6-$^{t}L_3$-A_9-V-A_9-$^{t}L_3$-K_6	2,4,6,8	25/50/75/100	3801.83	950.88	760.90	634.26	543.79	475.94	951.00	761.00	635.00	544.00	476.00
W-K_6-$^{t}L_3$-A_9-V-A_9-$^{t}L_3$-K_6	2,3,5,6,7	20/40/60/80/100	3802.84	951.13	761.11	634.42	543.93	476.07	952.00	761.00	634.00	544.00	476.00
W-K_6-$^{t}L_3$-A_9-V-A_9-$^{t}L_3$-K_6	8,12,14,16,18	20/40/60/80/100	3802.84	951.13	761.11	634.42	543.93	476.07	952.00	761.00	634.00	544.00	476.00
W-K_6-$^{t}L_3$-A_9-V-A_9-$^{t}L_3$-K_6	11,13,15,17,19	20/40/60/80/100	3802.84	951.13	761.11	634.42	543.93	476.07	952.00	761.00	634.00	544.00	476.00

IV. CD ellipticities, which have corroborative value, are unsuited as primary tools for the assignment of helical propensities from host-guest mutants.

A. Experimental circular dichroism characterization of helix-coil peptide equilibria; variability of helical structure; structural-dependences of the helical circular dichroism ellipticity $[\theta]_{222,H,n,T}$

For a typical peptide the proximity-coupled $\pi\rightarrow\pi^*$ and $n\rightarrow\pi^*$ electronic and magnetic transitions of its backbone amides define the major CD chromophores within the wavelength region of 185 to 250 nm. Mean values of ϕ and ψ dihedral angles, which fall within Ramachandran-allowed regions, define the signs and intensities of these transitions,[1] and for peptides in solution, CD ellipticities thus provide a unique tool for conformational assignments. The distinctive signature of the α-helical conformation is an intense positive ellipticity maximum near 290 nm, and a pair of intense negative ellipticity minima at 208 and 222 nm.

$$[\theta]_{222,Exper,n,T} = FH\,[\theta]_{222,H,n,T} + (1 - FH)\,[\theta]_{222,C,n,T} \quad Y\ FH\ [\theta]_{222,H,n,T} \qquad (1)$$

$$[\theta]_{222,H,n,T} = [\theta]_{222,H,\infty,T}\,(1 - X/n) \qquad 0 \leq X \leq 1.0 \qquad (2)$$

With increasing temperature, a helical peptide in water that is unassociated and lacks stabilization from tertiary packing undergoes reversible helix-coil melting, characterized by a decrease in the mole fraction FH of its helical residues and a proportionate increase in the mole fraction (1 − FH) of residues that assume coil conformations. Given Equation (1) parameter values, one can to a good approximation characterize helix-coil melting from the experimental temperature dependence of the 222 nm molar per-residue ellipticity $[\theta]_{222,Exper,n,T}$, and the accuracy of this two-state model can be confirmed for a particular peptide by ellipticities at 203 nm, at which coil and helix values are equal.[2] *The model is confirmed if the T-dependent CD spectra share a 203 nm isodichroic point.*[3] At one or more fixed temperatures, Eequation (1) is also universally used to assign FH changes induced by a series of guest residue substitutions within a host helical peptide. However the single reported 203 nm test of the valididity of this use failed to yield consistent isodichroic behavior.[4]

For either FH calculation, accurate assignments for the helicity parameters are essential, and the major issue explored in this supplement section is their accuracy when applied to host-guest data. Although the $[\theta]_{222,H,n,T}$ and $[\theta]_{222,H,\infty,T}$ parameters resemble UV-vis spectroscopic extinction coefficients, they differ in two fundamental respects: their intensities reflect the local structural environment, and they are temperature-sensitive.[3,5.6]

The structural variability of the α-helix itself accounts for much of this sensitivity. An α-helical conformation is defined by a contiguous sequence of backbone C=O to H-N amide hydrogen bonds of the 3.6_{13} type, and modeling as well as examples from the PDB show this structural condition to be met provided the average of sums of α-carbon ϕ, ψ pairs within the sequence lies close to −105°.[7] However, within this constraint, ϕ ranges from − 25 to − 95°, with corresponding ψ values of − 80 to − 10°.[7] Molecular modeling of polyalanines reveals the Ramachandran helical region as an extended ϕ, ψ trough, with shallow local minima, that spans these ϕ, ψ ranges.[8] Moreover ab initio CD modeling shows that this α-helical ϕ-angle variation results in a substantial intensity change for $[\theta]_{222,H}$,[9] and experimental data support this prediction. Mean values for $[\theta]_{222,H,\infty,T}$ of PDB α-helices, which have a mean ϕ of − 63°,[10] fall within the range, $-37x10^3$ to $-44x10^3$ deg cm^2 dm^{-1}, also consistent with length extrapolations from alanine-rich heteropeptide CD data.[6] A different picture emerges from our NMR and CD studies of core regions of N- and C-capped, fully helical polyalanine cores.[11] Their ϕ is -51 ± 2°, close to an average of values for the classic fiber-diffraction structure and the Pauling α-helix, and their $[\theta]_{222,H,\infty,T}$ is $-(60.5 \pm 1.3)x10^3$ deg cm^2 dm^{-1}, confirmed by low temperature CD spectra of a winter flounder protein with a 70 % Ala content).[12]

The 3_{10} helix, frequently detected within short helical regions of PDB globular proteins, is more tightly helical than the α, with ϕ = − 49°, ψ = − 25°,[13] and novel ESR[14] and NMR[15] structural methods, applied to a range of test peptides, demonstrate hybrid 3_{10}-α character that is most pronounced within end regions. Peptides with pure 3_{10} structure are characterized by exceptionally weak intensities for $[\theta]_{222,H}$, although shorter wavelength CD maxima and minima have nearly normal intensities.[16] Doubt clearly compromises compromises accuracy for FH values assigned from $[\theta]_{222,Exper}$ values of peptides that, like these, assume hybrid 3_{10}–α structures.

B. Evidence for significant perturbations of the intensity of $[\theta]_{222,H}$: The end-region correction of Equation (2). Plausible corrections in $[\theta]_{222,H,\infty,T}$ from ^{13}C=O NMR chemical shift data of mutants **1** and $[\theta]_{\lambda,Exper,n,T}$ data of mutants **2**; Tests of the validity of the two-state assumption of Equation (1) from $[\theta]_{203}$ data. In the accompanying manuscript we report a set of temperature-dependent relative helical propensities w_{Xxx}/w_{Ala} assigned from $[\theta]_{222,Exper,n,T}$ data for a mutant series **2** and a second propensity set assigned from ^{13}C=O NMR chemical shifts for a mutant series **1**. Although statistical tests yield satisfactory correlations for this w_{Xxx}/w_{Ala} pair, the magnitudes for many of the ellipticity-derived w_{Xxx}/w_{Ala} are smaller than those derived from shifts. We now make the case that the likely

cause is a reduction in the intensity of $[\theta]_{222,H,\infty,T}$, caused by central (Ala → Guest) replacements that perturb local helical structure.

A special problem potentially compromises accuracy for helical propensities derived from ellipticity data. For a sequence that contains n alanine residues and a single central guest, the fractional helicity FH is a global parameter that equals the average of $n + 1$ site helicities FH_i. We have previously shown that as measures of helix-coil sequence equilibria, the FH and any of the FH_i are fully equivalent,[17] but practically speaking, the FH_i are much more versatile. From a full list of FH_i one can exclude the FH_i that correspond to sites most susceptible to spurious perturbations, and as shown in the main text, these include sites within end regions as well as sites locally N-terminal to the guest. For a given peptide, a single $[\theta]_{222}$ is measurable, and it yields only one FH value.

A structure- and solvation-induced ellipticity perturbation is clearly embodied in the empirically characterized parameter X that appears in Equation (2), which is universally used to assign a length-dependence to $[\theta]_{222,H,n,T}$ from the length-independent core ellipticity $[\theta]_{222,H,\infty,T}$. Since X invariably has a positive value, inspection of Equation (2) shows that a residue at or near an N- or C-terminus must contributes less to $[\theta]_{222,H,n,T}$ than a core residue.[18]

We have clarified these issues experimentally.[11] For a tailored length series, $10 \leq n \leq 23$, of spaced, solubilized polyalanines with exceptional helicities, the ^1H and ^{13}C NMR chemical shifts of the helical backbone residues of the two sets of four N- and C-terminal residues are strongly site-dependent, but backbone shifts for the remaining $(n - 8)$ core residues have fixed values, independent of site or length n, and their FH values[19] exceed 0.99.

$$[\theta]_{\lambda,H,n,T} = ([\theta]_{\lambda,H,\,core,Molar} + [\theta]_{\lambda,H,\,caps,\,Molar})/n = ([\theta]_{\lambda,H,\infty,T}(n - k) + [\theta]_{\lambda,H,\infty,T}(k - X))/n \qquad (2a)$$

$$[\theta]_{222,H,caps,T}/[\theta]_{222,H,\infty,T} = (k - X)/k \qquad (3)$$

It is conceptually useful to define a new parameter k as the number of non-core residues within a helical peptide, incorporating it into Equation (2a). (Inspection shows this to be a full equivalent of Equation (2).) For our polyalanine series, k equals 8. For each series member, the intensity of $[\theta]_{\lambda,Exper,n,T}$ was measured and expressed in molar units. Their length regressions proved to be strictly linear at all wavelengths, within measurement error, the resulting λ-dependent slopes equal the core per-residue molar ellipticities $[\theta]_{\lambda,H,\infty,T}$, and multiplication by the core length $(n - k)$ yields molar ellipticities that correspond to the first term of Equation (2a). The second term is $[\theta]_{\lambda,H,\infty,T}(k - X)$, which equals $[\theta]_{\lambda,H,\,caps,\,Molar} = k\,[\theta]_{\lambda,H,\,caps}$. This is defined experimentally as the intercepts of the

regression. If one divides the value of the intercept at 222 nm by k and regroups terms, Equation (3) results.

This equation expresses the relative decrease of per-residue ellipticity within non-core regions as a simple function of X and k. From three assigned X values,[5,11,20] we calculate the range at 2 °C for $[\theta]_{222,H,caps,T}/[\theta]_{222,H,\infty,T}$ as 0.7 to 0.3. Expressed as a penalty percentage, it corresponds to the decrease in $[\theta]_{222}$ intensity that results if one imagines that one completely helical alanine from the core is transferred to an average site within the end regions. This decrease lies between 30 and 70 % of the core value; it is strongly sensitive to cap structure.[21]

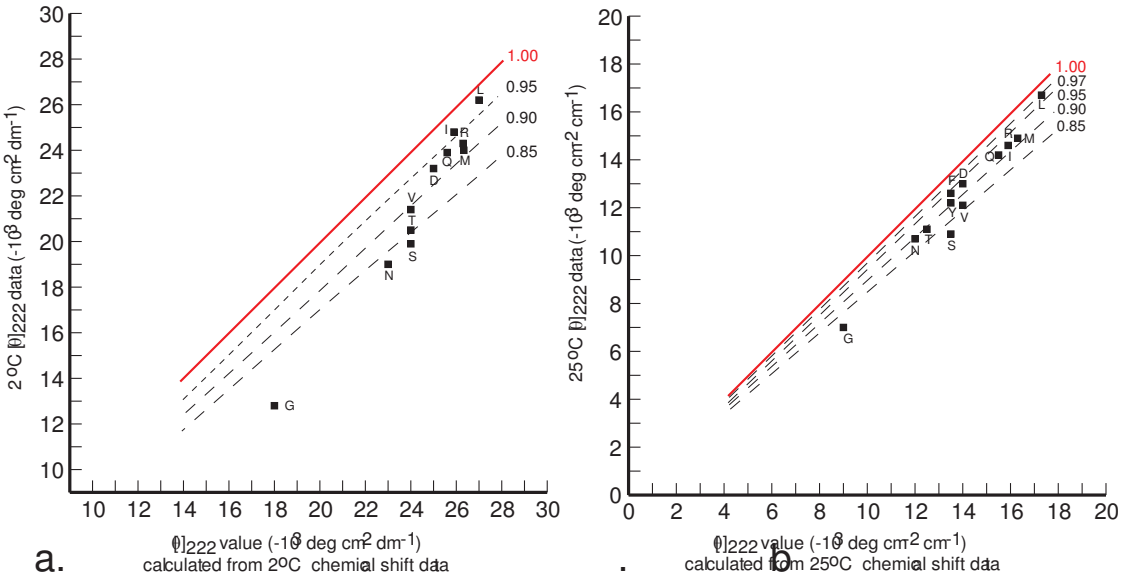

Figure 1 Value axis squares show experimental values of $[\theta]_{222,Exper,n,T}$ for mutants ^{t}L-Ala$_9$Xxx Ala$_9$-^{t}L at 2 °C (a) and 25 °C (b). These are plotted parametrically vs. $[\theta]_{222,n,T}$ values that are Lifson-Roig calculated from relative helical propensities w_{Xxx}/w_{Ala} assigned in the accompanying report from ^{13}C=O chemical shifts. The dotted lines in each graph correspond to $[\theta]_{222,n,T}$ values from a series of calculations using the helical propensity as an independent variable with the range 0.05 to 1.0; for the series, the value of $[\theta]_{222,H,\infty,T}$ (Equation 2) was multiplied by an attenuating factor within the range 0.97 to 0.85. The red lines show correlations for identical w_{Xxx}/w_{Ala} sets.

What fractional reductions in the value of $[\theta]_{222,H,\infty,T}$ would be required to generate consistent w_{Xxx}/w_{Ala} sets from both shift and ellipticity data of Figure 5 of the main text? Figure 1 addresses this question. The vertical displacements of the black squares correspond to the $[\theta]_{222,Exper,n,T}$ data measured at 2 °C and 25 °C for guests Xxx that yield deviant w_{Xxx}/w_{Ala} values. The horizontal

displacements of the squares correspond to $[\theta]_{222}$ values modeled from propensities assigned from $^{13}C{=}O$ chemical shift data, as described in the accompanying text, using the host-derived value of $[\theta]_{222,H,\infty,T}$. The dotted black lines show modeled values of $[\theta]_{222}$ calculated from $[\theta]_{222,H,\infty,T}$, attenuated by successive factors 0.97, 0.95, 0,90, or 0.85. Inspection shows that with the exception of Xxx = Gly, all ellipticity data can be modeled attenuations within this plausible range. The glycine result deserves comment. Previously reported relative helical propensities for glycine span a fifteen-fold range, and assignments from ellipticity data cluster at the lower end.[22] The Ramachandran permissiveness of a Gly residue strongly suggests that, within a peptide sequence, glycine may be uniquely tolerant of 3_{10} structure, implying that the appropriate values of $[\theta]_{222,H,\infty,T}$ for helicity data of glycine mutants must be lower than normal, with a corresponding underestimation of the glycine propensity.[23]

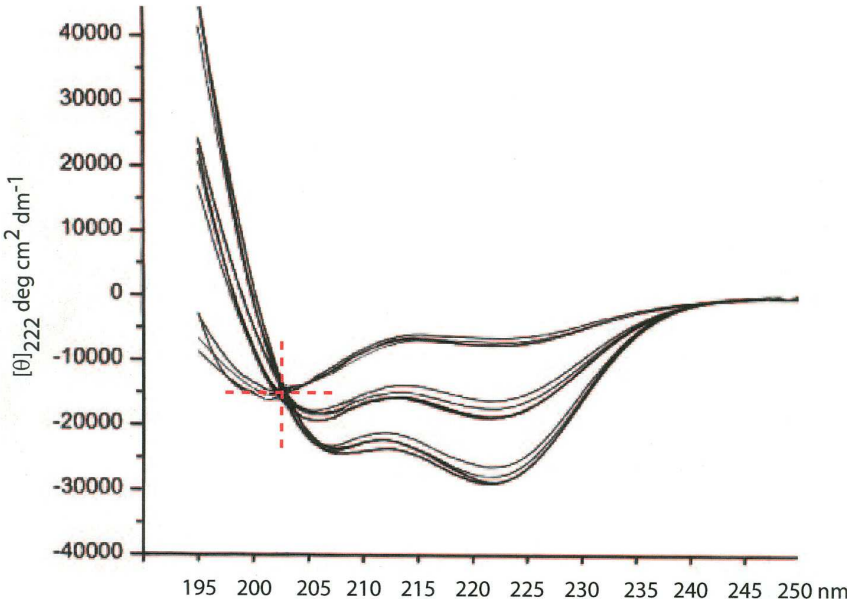

Figure 2 CD spectra, 190 to 250 nm, at 2, 25, and 60 °C, for the host peptide ^{t}L-Ala$_{19}$-^{t}L and for mutants ^{t}L-Ala$_9$XxxAla$_9$-^{t}L, Xxx ≡ Nle (norleucine), Nva (norvaline), and Abu (α-aminobutyric acid). A well-defined isodichroic point is evident at 202.5 °C with $[\theta]_{2025,Exper} = (-15 \pm 1)x10^3$ deg cm^2 dm^{-1}, consistent with values reported by Holtzer and Holtzer.[2] The two error assignments lie within precision limits.

An independent test for accuracy examines mutant ellipticities measured at 203 nm. The guest-dependent, corrected values $[\theta]_{222,H,\infty,T}$ that appear in Figure 1 were assigned under the assumption that a wrong choice for this parameter is wholly responsible for the deviations that appear within

Figure 5 of the main text. If this assumption is correct, corresponding guest-dependent deviations should appear if one compares mutant values for $[\theta]_{203}$. (The data points of Figure 1 show only the deviant values; no deviations were detected for mutants derived from the non-natural residues Nva and Nle, which bear straight-chain alkyl side chains.) Figure 2 shows superimposed CD spectra measured at 2, 25, and 60 °C for the host peptide ^{t}L-Ala$_9$XxxAla$_9$-^{t}L, Xxx ≡ Ala for a homologous series of three mutants containing site 10 Abu,[24] Nva, or Nle residues. The twelve CD spectra of Figure 2 exhibit a well-defined isodichroic point at 202.5 nm, with an ellipticity intensity of -15 x10^3 deg cm^2 dm^{-1}, fully consistent with an authoritative literature assignment.[2]

A different picture results if includes in Figure 2 the 2, 25, and 60 °C CD spectra of mutants derived from guests Val, Ile, Met, and Phe. The limits of curve intersections broaden to a wavelength range of 201 to 205 nm, and at 202.5 nm, the error in the ellipticity increases to ± 3x10^3 deg cm^2 dm^{-1}, corresponding to a ± 20 % relative error, which lies outside data precision limits. A plot of 2, 25, and 60 °C CD spectra of mutants derived from guests Gln, Asn, Ser, Met, Thr, Tyr, Asp, and Glu yields curve intersections that expand to a wavelength range of 200 to 209 nm, and at 202.5 nm, the error in the ellipticity increased to ± 5x10^3 deg cm^2 dm^{-1}, corresponding to a ± 33 % relative error. These findings definitively validate our conclusion that guest-induced ellipticity perturbations are large enough to explain the accuracies seen in Figure 1. For a majority of the natural amino acid residues, we have proved that CD measurements are unsuitable tools for assigning primary values for host-guest derived helical propensities.

Useful supporting information is also provided by comparisons with double mutant sets as seen in the following table.

Table I0. Correlations Between Paired w_{Xxx}/w_{Ala} Sets. Xxx = A, L, M, I, Q, V, F, Y, S, N, T, G Set A: w_{Xxx}/w_{Ala} Assigned from $^{13}C{=}O$ Chemical Shifts at Site 14 of Mutants **1**. Set B: w_{Xxx}/w_{Ala} Assigned from $[\theta]_{222}$ Values of Mutants **2**. Set C: w_{Xxx}/w_{Ala} Assigned from $[\theta]_{222}$ Values of Mutant **2** analogs that contain Two Xxx guests at Sites 10 & 11.

T, °C	Paired Sets	Slope	Intercept	Fit (SD)	CC	Mean Δ %
2	A - B	1.01	− 0.15	0.08	0.95	+ 41
2	A - C	0.99	− 0.11	0.06	0.97	+ 30
2	C - B	0.95	+ 0.05	0.03	0.99	+ 11
25	A – B	0.96	− 0.09	0.06	0.97	+ 25
25	A – C	0.83	+ 0.01	0.07	0.95	+ 11
25	C – B	0.87	+ 0.08	0.03	0.99	+ 14
60	A – B	0.99	+ 0.06	0.08	0.89	− 8
60	A – C	0.81	+ 0.18	0.04	0.96	− 8
60	C – B	0.64	+ 0.27	0.07	0.84	+ 0.6

V. References

(1) Yang. J. T.; Wu, C.-S. C.; Martinez, H. M. *Methods Enzymol.* **1986**, *130*, 208—269.

(2) Holtzer, M. E.; Holtzer, A. *Biopolymers* **1992**, *32*, 1675—1677**.**

(3) Wallimann, P., Kennedy, R. J., Miller, J. S., Shalongo, W., Kemp, D. S. *J. Am. Chem. Soc.* **2002**, *125*, 1203—1220.

(4) Lyu, P. C.; Liff, M. I.; Marky, L. A.; Kallenbach, N. R. *Science* **1990**, *250*, 669—673.

(5) Job, G. E.; Kennedy, R. S.; Heitmann, B.; Miller, J. S.; Walker, S. M.; Kemp, D. S. *J. Am. Chem. Soc.* **2006**, *128*, 8227—8233.

(6) Luo, P.; Baldwin, *Biochemistry* **1997**, *36*, 8422—8421.

(7) Besley, N. A.; Hirst, J. D. *J. Am. Chem. Soc.* **1999**, *121*, 9636—9644.

(8) Mahadevan, J.; Lee, K.-H.; Kuczera, K. *J. Phys. Chem. B* **2001**, *105*, 1863—1976.

(9) Woody, R.W.; Sreerama,N. *J. Chem. Phys.* **1999**, *111*, 2844—2845. Manning, M. C.; Woody, R.W. *Biopolymers* **1991**, *31*, 569—586.

(10) Barlow, D. J.; Thornton, J. M. *J. Mol. Biol.* **1988**, *201*, 601—619.

(11) Heitmann, B.; Job, G. E.; Kennedy, R. S.; Miller, J. S.; Walker, S. M.; Kemp, D. S. *J. Am. Chem. Soc.* **2005**, *127*, 1690—1704.

(12) Marshall, C. B., Chakrabartty, A., Davies, P. L. *J. Biol. Chem.* **2005**, *280*, 17920—17929.

(13) Creighton, T. R. "Proteins: Structure and Molecular Properties", W. H. Freeman and Co., New York, 1983, p 171.

(14) Bolin, K. A.; Millhauser, G. L. *Acc. Chem. Res.* **1999**, *32*, 1027—1033.

(15) (a) Millhauser, G. L.; Stenland, C. J.; Hansen, P.; Bolin, K. A.; van de Ven, F. J. M. *J. Mol. Biol.* **1997**, *267*, 963—974; (b) Long, H. W.; Tycko, R. *J. Am. Chem. Soc.* **1998**, *120*, 7039—7048.

(16) Toniolo, C.; Polese, A.; Formaggio, F.; Crisma, M.; Kamphuis, J.; *J. Am. Chem. Soc.* **1996**, *118*, 2744—2745.

(17) Nasr, K. A.; Schubert, C. R.; Török, M.; Kennedy, R. J.; Kemp, D. S. *Biopolymers* **2009**, *91*, 311—320.

(18) A rigorous distinction between core and ends is justified by the rigid cylindrical structure of a peptide helix. Since for an unaggregated homopeptide sequence of sufficient length, energy perturbations are plausibly all local, and a core must exist in which all residues have the same structure, helix-coil energetics, and per-residue ellipticities. This convergence defines $[\theta]_{\lambda,H,\infty,T}$.

(19) Assigned from NH → ND kinetics at 2 °C.[11]

(20) Walker, S. M; Kemp, D. S. unpublished observations.

(21) For the cap-stabilized polyalanines of reference 11, $X = 2.5$; for the peptides **1**, which contain bulky, hydrophobic ^{t}L spacing regions, $X = 6$ to 7, and $X = 4$ to 5 for corresponding peptides containing alanine and D-alanine spacers, Kennedy, R. S.; Miller, J. S.; Walker, S. M.; Kemp, D. S. *J. Am. Chem. Soc.* **2005**, *127*, 16961—16968.

(22) Luo, P.; Baldwin, R. L.; *Proc, Natl. Acad. Sci. USA* **1999**, *96*, 4930—4935.

(23) Lee, J.; Kemp, D. S. unpublished observations.

(24) The required synthetic facilities and personnel were no longer available to us for synthesis of a mutant **1** that contains ^{13}C=O reporters and a site 10 Abu = α-aminobutyric acid guest.